ELSEVIER

Biochimica et Biophysica Acta 1514 (2001) 280–290

BIOCHIMICA ET BIOPHYSICA ACTA
BBA

www.bba-direct.com

The effect of cholesterol in a liposomal Muc1 vaccine

Michael M. Batenjany *, Lawrence T. Boni, Yuqing Guo, Mary E. Neville, Shalini Bansal, Richard J. Robb, Mircea C. Popescu

Biomira USA, Inc., 1002 Eastpark Boulevard, Cranbury, NJ 08512, USA

Received 18 January 2001; received in revised form 26 June 2001; accepted 28 June 2001

Abstract

A liposomal Muc1 mucin vaccine for treatment of adenocarcinomas was formulated by incorporating a synthetic Muc1 mucin-based lipopeptide and Lipid A into a DPPC/cholesterol bilayer. Vaccination of mice with the liposomal formulation produced a peptide-specific immune response dependent on the cholesterol content. The response occurred at a threshold of 20–23 mol% cholesterol, and was optimal at cholesterol levels of ≥ 30 mol%. To understand this cholesterol dependency, we studied the effect of cholesterol on the liposomal bilayer and surface properties. Freeze-fracture electron microscopy showed a unique surface texture that was codependent upon cholesterol (≥ 20 mol%) and lipopeptide content. Fluorescence anisotropy measurements exhibited a significant decrease in the rotational motion of 1,6-diphenyl-1,3,5-hexatriene in formulations containing > 20 mol% cholesterol and only in the presence of the lipopeptide. At 20 mol% cholesterol and with lipopeptide, DSC showed a significant increase in the main phase transition of the DPPC bilayers, while Raman spectroscopy indicated a more ordered arrangement of DPPC molecules compared to control liposomes containing DPPC/cholesterol alone. Taken together, the data suggest the presence of lipopeptide-rich microdomains at and above a threshold of 20 mol% cholesterol that may play a role in the induction of a peptide-specific immunological response.

Keywords: Cholesterol; Liposome; Mucin-based lipopeptide; Vaccine; Lipid A

1. Introduction

Cholesterol is the most studied sterol in animal tissue and a significant component affecting many cellular and artificial membrane properties. Cholesterol has been included in many liposomal formulations because of its effects on the bilayer's physical parameters, as well as its biochemical interactions with membrane constituents. Within the membrane, cholesterol may associate with particular lipids or proteins, regulate bilayer fluidity, and induce a condensing effect which decreases membrane permeability and increases rigidity [1].

Various biological responses have been attributed to the association of cholesterol with other membrane components and its affects on the bilayer properties within liposomal and cellular membranes. These have included the formation of lipid rafts [2], an enhanced primary immune response [3], activation of complement by liposomes [4], microviscosity

* Corresponding author. Fax: +1-609-655-1755.
E-mail address: mbatenjany@biomira.com (M.M. Batenjany).

0005-2736/01/$ – see front matter
PII: S0005-2736(01)00383-2

changes affecting antigen displacement and tumor antigenicity [5,6] and influencing the functional properties of receptor proteins by formation of populations of high and low affinity receptors [7]. Thus, the presence of cholesterol-dependent microdomains and their effects on the membrane microviscosity can have very significant physiological effects.

Similar to the above examples, we have also noted a cholesterol dependency on the immune responses induced by a multilamellar liposomal vaccine formulated for immunotherapeutic use against adenocarcinomas [8–13]. The vaccine was composed of DPPC/DMPG/cholesterol and contained a synthetic, palmitated human Muc1 mucin-based peptide (BLP25) and Lipid A. In murine models, this formulation induced antigen-specific T-cell proliferation and cytokine (interferon (IFN)-γ) secretion. Moreover, in normal and human Muc1 transgenic mice, vaccination with the formulation protected against challenge with syngeneic tumors transfected to express human Muc1 and decreased the rate of growth of established tumors. This formulation is currently in clinical trials for lung cancer.

During preclinical studies, it was noted that the biological efficacy of this liposomal Muc1 vaccine and a similar formulation lacking DMPG were dependent on the amount of cholesterol included in the liposomal formulation. To investigate the biophysical basis of the latter observation, we have studied the effects of varying amounts of cholesterol on DPPC bilayers in the presence and absence of Muc1 lipopeptide and Lipid A. We report evidence of changes within the liposomal membrane, co-dependent upon cholesterol and lipopeptide. We discuss these changes and suggest that they are consistent with cholesterol/lipopeptide-rich microdomains that may be important for biological activity.

2. Materials and methods

2.1. Materials

The synthetic, palmitated 27-amino-acid Muc1 mucin-based lipopeptide (STAPPAHGVTSAPDTRPAPGSTAPP-K(Pal)G; referred to as Muc1 lipopeptide) and an irrelevant peptide (EAIQPGCIGGPKGLPGLPGP; referred to as BP-072) were synthesized by Biomira (Edmonton, AL, Canada) [12,13]. 1,2-Dipalmitoyl-*sn*-glycero-3-phosphocholine (DPPC), Lipid A, cholesterol and sodium dodecyl sulfate (SDS) were purchased from Avanti Polar Lipids (Alabaster, AL). 1,6-Diphenyl-1,3,5-hexatriene (DPH) was purchased from Molecular Probes (Eugene, OR). Trifluoroacetic acid was purchased from Burdick and Jackson (Muskegon, MI). Absolute ethanol (200 Proof) was U.S.P. grade and purchased from Quantum Chemical Co. (Tuscola, IL). Sterile 0.9% normal saline solution (NSS) for injection (U.S.P.) was purchased from Abbott Laboratories (Chicago, IL). Sterile filtration was performed using Millex-GV, 0.22-μm, 13-mm filter units from Millipore (Bedford, MA). Lyophilization was performed in 2-ml (13-mm), U.S.P. grade, Type I glass vials from Wheaton (Millville, NJ).

2.2. Preparation of liposomal Muc1 vaccine

A liposomal vaccine formulation for human mucin-1 was prepared by incorporating a Muc1 mucin lipopeptide into a DPPC/cholesterol bilayer. Lipid A was included as an adjuvant. The appropriate stock reagents of DPPC, cholesterol, Muc1 lipopeptide and Lipid A were warmed to 55°C in a water bath for 15–20 min. The required amount of each component was added to a clean stoppered 2-ml glass vial, which was vortexed briefly (3 s×7 times) and returned to the 55°C water bath. Water (55°C) was added to the vial at a solvent/water ratio of 9:1 by volume and the mixture vortexed briefly as above. The mixture was returned to the 55°C water bath for about 15–20 min, vortexing (as above) twice during that period. Samples were lyophilized using a Dura-Stop MP shelf lyophilizer (FTS Systems, Stone Ridge, NY) or a Model SC110 SpeedVac (Savant Instruments, Holbrook, NY). Freeze-dried formulations were hydrated by addition of sterile NSS solution at 55°C with brief vortexing. After hydration, preparations typically contained 20 mg/ml total bulk lipid (e.g., DPPC and cholesterol), 400 μg/ml Muc1 lipopeptide and 200 μg/ml Lipid A.

2.3. Differential scanning calorimetry (DSC)

DSC runs were performed on a CSC 4100 Multicell Differential Scanning Calorimeter (Calorimetry

Sciences Corp., Provo, UT). Scan rates were run at 20°C/h. NSS was used for baseline subtraction. Baseline subtraction, correction for the thermal instrument response and conversion to heat capacity (μJ/°C) as a function of temperature was performed using software supplied by CSC. The calorimetric data were imported into Grams/32, v.5.0 (Galactic Industries Corp., Salem, NH) for baseline and offset correction, smoothing and plotting. Data were not smoothed or only minimally smoothed by using a Savitsky–Golay smoothing routine. This method uses a convolution approach and performs a least squares fit to a specified window. When data were smoothed, a third-order polynomial and a window of 5–11 data points was typically employed.

2.4. Raman vibrational spectroscopy

Samples were placed in a glass capillary and spun for 15 min in a microcapillary centrifuge to pack the sample. The capillary was then sandwiched between a heat exchanger and a peltier wafer (Melcor Electronic Products, Trenton, NJ). Temperature control was via a Model TC2 Peltier Controller (Alpha Omega Instruments, Johnston, RI). Samples were run at 19°C (±0.2°C). Raman spectra were recorded on a Spex Ramalog-131 dispersive spectrometer equipped with a Model 1403P motorized double monochrometer and a Spex Spectrum One CCD detector (Spex Industries, Edison, NJ). An Innova Model 90 argon laser (Coherent, Santa Clara, CA) provided 150–200 mW of 514.5 nm laser excitation to the sample. At 150–200 mW no significant laser heating effects were observed. Typically, ten spectra were coadded using a time constant of 16 s per collection. Spectral resolution was at $\sim$1 cm^{-1}.

2.5. Sizing of the liposomal Muc1 vaccine

The liposomes were sized using an Accusizer 770 from Particle Sizing Systems (Santa Barbara, CA). The binning was set at 128 diameter channels, the threshold was set to 0.99 μm and baselines were obtained at the beginning of each session by using NSS. Typically, 20–25 μl of the hydrated preparation was added to 50 ml of NSS in the round-bottom reservoir of the Accusizer 770. NSS solution was used as the diluent with continuous stirring.

2.6. Quantification of Muc1 lipopeptide by high-pressure liquid chromatography (HPLC)

The samples were analyzed for total Muc1 lipopeptide and free Muc1 lipopeptide (supernatant after centrifugation at 12 000×*g* for 30 min at 4°C). Prior to injection samples were diluted 1:9 (total) or 1:1 (supernatants) by volume in a methanol solution containing 30% (v/v) TFA and 2.5% (w/v) SDS. Injection (40 μl = 1 μg Muc1 lipopeptide) was made onto a 25 cm×4.6 mm reverse-phase column (C_4) with a 300-Å pore size (Vydac, Hesperia, CA). The column was mounted in a Waters Model 625 LC (Milford, MA) equipped with a Waters Variable Wavelength Detector #486 set to 206 nm. Samples were run using a gradient from 60% perchloric acid (0.1 M, pH 2.5)/40% acetonitrile to 10% perchloric acid (0.1 M, pH 2.5)/90% acetonitrile over 26 min. Analysis was performed using Millennium software (Waters, version 2.00) and based on a standard curve generated over the range of 0.1–2.0 μg Muc1 lipopeptide. Recovery was based on theoretical expectations and incorporation was determined from differences between the total amount of Muc1 lipopeptide in the samples and the amount found in the supernatants.

2.7. Analysis of components by thin-layer chromatography (TLC)

Cholesterol and Lipid A concentration in the liposomal Muc1 vaccine (i.e., hydrated product) was determined by TLC. Samples were dissolved in chloroform/methanol (2:1) to form an optically clear solution. This solution (2–100 μl) was loaded by capillary action onto 20×20-cm Whatman (Clifton, NJ) silica gel plates (250 μm thick, 19 channel prescored, 60 A mesh size). Developing tanks were equilibrated for 2 h at room temperature before adding the plates. The system was run until the solvent front was 2 cm from the top of the plate (about 30–45 min). The following mobile phases were used at the indicated volume to volume ratios: (1) chloroform/methanol/water/ammonium hydroxide (50:25:4:2) for Lipid A detection; (2) hexane/diethyl ether/formic acid (40:10:1) for cholesterol detection. Plates were removed from the developing tanks and allowed to air dry at room temperature then dipped for 5–10 s

into a copper(II) sulfate reagent (0.63 M $CuSO_4$ in 1.2 M H_3PO_4). After allowing excess reagent to drain off the plate, the spots were visualized by heating the plate 5 or more minutes in a 160°C oven. Sensitivity was submicrogram ($\sim$0.25 μg can be easily seen).

2.8. Fluorescence anisotropy measurement

Liposomal preparations were first adjusted to about 0.5 mM total bulk lipid (DPPC and cholesterol), then 1,6-diphenyl-1,3,5-hexatriene (DPH; 0.861 mM stock solution in ethanol) was added to a molar ratio of total bulk lipid/DPH of approximately 500:1. Anisotropy measurements were performed using a PTI QM-1 Fluorometer (Photon Technology International, Monmouth Jct., NJ) equipped with a thermojacketed cell holder and L-format Glan–Thompson polarizers. Temperature was accurate to ±1°C. Readings were obtained at 22°C, 41°C and 50°C using four different polarizer positions (VV, VH, HH, HV). After samples were equilibrated at the appropriate temperatures for 30 min, data was collected using the FeliX Timebased Acquisition Mode (PTI software) with excitation wavelength at 350 nm, emission wavelength at 430 nm and a duration of 60 s. The instrumental G-factor ($\sim$0.5) was calculated each time, then using the mean emission values, the fluorescence anisotropy (r) was calculated as follows:

$$G = I_{HV}/I_{HH};\ r = (I_{VV} - G(I_{VH}))/(I_{VV} + 2G(I_{VH}))$$

or

$$r = (I_{VV}I_{HH} - I_{VH}I_{HV})/(I_{VV}I_{HH} + 2I_{VH}I_{HV})$$

2.9. Analysis of P_i content

Preparations of the liposomal Muc1 vaccine were analyzed for phospholipid content using the ashing method of Ames [14]. All samples and standards were run in triplicate. Optical densities were obtained at 820 nm using a Model UV-160U UV-Vis spectrophotometer from Shimadzu Corp. (Tokyo, Japan). Lots of Lipid A were also assayed to test their expected molar P_i content.

2.10. Electron microscopy of the liposomal Muc1 vaccine

The morphology of liposomal Muc1 vaccines were studied using freeze-fracture electron microscopy. Samples were quick-frozen in liquid propane then fractured and replicated on a Balzers (Liechtenstein) freeze-etch unit, under a vacuum of better than 1×10^{-6} mbar and a temperature of −115°C. Micrographs of the replicas were obtained using a Philips Model 300 electron microscope (The Netherlands).

2.11. Immunization of mice with the liposomal Muc1 vaccine and IFN-γ secretion

C57BL/6 female mice (8–11 weeks old) from Taconic Farms (Germantown, NY) were immunized with the liposomal Muc1 vaccine. In four independent experiments, the vaccine was administered in two 50-μl subcutaneous injections in the inguinal region. In each experiment, nine mice per group were used. After nine days, the mice were sacrificed by cervical dislocation and lymph nodes and spleens were collected. For each group of nine mice, lymphocytes were isolated from three subsets, each representing the pooling of three mouse spleens or inguinal lymph nodes. These lymphocytes were restimulated in vitro for 72 h with Muc1 lipopeptide, an irrelevant peptide (BP-072), media, or concanavalin A (Con A). IFN-γ secretion into the culture supernatants was measured using an antibody-based microtiter plate capture assay. Europium-labeled streptavidin and time-resolved fluorometry on a Model 1232 Delfia Fluorometer (Wallac, Turku, Finland) were used for quantitation based on a standard curve of purified recombinant IFN-γ (BD PharMingen, San Diego, CA).

3. Results and discussion

3.1. Effect of cholesterol content on biological activity of the vaccine

The liposomal Muc1 vaccine was formulated with varying amounts of cholesterol (0–50 mol%) to determine the influence of cholesterol content on the immune response. Cholesterol is miscible in DPPC bilayers up to or greater than 50 mol% [15]. The

vaccine was administered by bilateral subcutaneous injection in the inguinal region. Lymphocytes were isolated from pooled inguinal lymph nodes and spleens (see Methods) and restimulated for 72 h in vitro with Muc1 lipopeptide, an irrelevant peptide (BP-072), media or Con A. The amount of IFN-γ released in the culture supernatant was quantitated and the mean and standard error of the data from four separate experiments is shown in Fig. 1. IFN-γ was not detected in control lymphocytes from mice that received saline or when any of the isolated lymphocytes were restimulated with an irrelevant peptide (data not shown), thus demonstrating that the response was antigen-dependent and antigen-specific. In addition, lymphocytes from mice inoculated with vaccine containing 0 or 10 mol% cholesterol did not produce IFN-γ upon restimulation in vitro. A small amount of IFN-γ was detected when the original vaccine contained 20–23 mol% cholesterol, but an optimal response occurred at cholesterol levels of 30–50 mol%. In control experiments (data not shown), it was demonstrated that the IFN-γ response

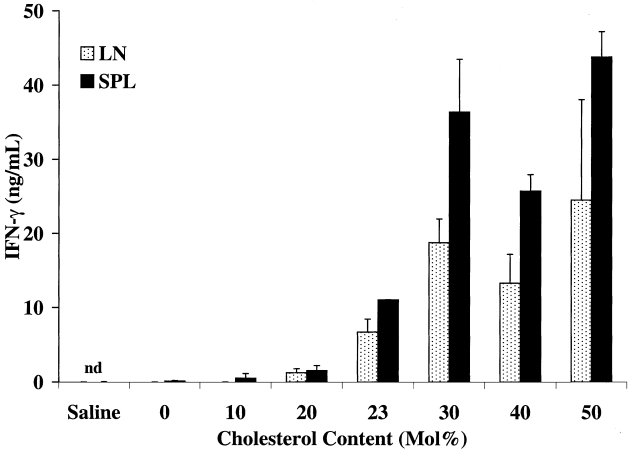

Fig. 1. IFN-γ response of mouse spleen and lymph node lymphocytes. The bars represent the means and standard error of data from four independent experiments in which mice were first vaccinated with liposomal formulations (20 mg/ml total lipid consisting of DPPC and cholesterol) containing Muc1 lipopeptide and Lipid A and different amounts of cholesterol. After 9 days, spleen and lymph node lymphocytes were restimulated in vitro with Muc1 lipopeptide and the amount of IFN-γ secreted was determined. No IFN-γ was detected in control mice receiving saline (nd, not detected) or when any of the isolated lymphocytes were restimulated in vitro with an irrelevant peptide (BP-072, data not shown).

was absolutely dependent upon inclusion of Lipid A adjuvant in the liposomal vaccine. Fig. 1 demonstrates that the release of IFN-γ, which varied with the cholesterol content of the vaccine, was both antigen-dependent and antigen-specific.

3.2. Surface morphology

Freeze-fracture electron microscopy was used to determine if the increase in the cholesterol content of the liposomal Muc1 vaccine correlated with any morphological differences. Fig. 2 exhibits the electron micrographs of formulations prepared at 0, 20, 30 and 50 mol% cholesterol. At ≥20 mol% cholesterol, a unique surface texture was observed when the Muc1 lipopeptide was included in the formulations (Fig. 2B–D). This surface appearance was not seen in freeze-fracture studies of formulations at 0 mol% cholesterol (Fig. 2A) or 10 mol% cholesterol (data not shown), nor was it seen in formulations at a higher cholesterol content (50 mol%) when the Muc1 lipopeptide was not included (Fig. 3B). In the absence of cholesterol (Fig. 2A), one of the vesicles exhibits the characteristic ripple phase of DPPC bilayers. In addition, the absence of Lipid A did not influence the liposomal surface texture (Fig. 3A). Hence, freeze-fracture electron microscopy demonstrated that a unique surface structure existed and was dependent upon a threshold of 20 mol% cholesterol and the presence of the Muc1 lipopeptide. The observed surface texture is likely a consequence of the fracture plane jumping between bilayers in the multilamellar vesicles. This could be caused by inhomogeneities within the plane of the bilayer and would be consistent with the presence of lipid microdomains. Moreover, the unique surface texture appeared to correlate with cholesterol levels required for induction of an immune response.

3.3. Bilayer characteristics

The fluorophore 1,6-diphenyl-1,3,5-hexatriene (DPH) was used to elucidate changes in the membrane order in the Muc1 lipopeptide vaccine which might shed light on the origin of the cholesterol-dependent surface morphology and immune response. Measurements were conducted at 22°C, 41°C and 50°C. These temperature points are significant for

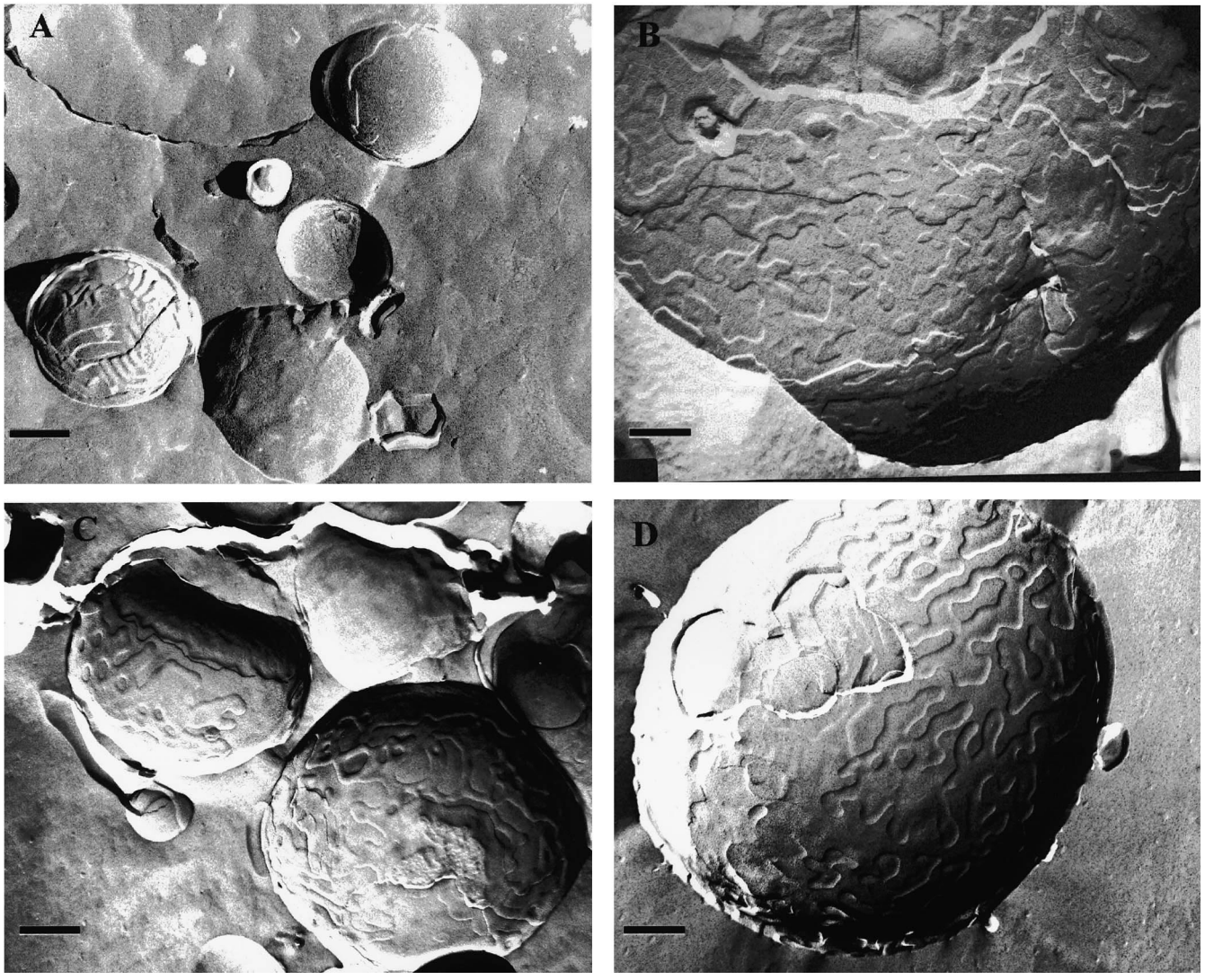

Fig. 2. Freeze-fracture electron micrographs of liposomal formulations. The cholesterol content of all the liposomal formulations was varied: 0 mol% (A); 20 mol% (B); 30 mol% (C); 50 mol% (D). All formulations contained 400 μg/ml Muc1 lipopeptide and 200 μg/ml Lipid A. Freeze-fracture was performed on formulations warmed to room temperature. Bar = 250 nm.

hydrated DPPC bilayers in that they represent the gel phase (22°C), the ripple/liquid-crysalline phase interface (41°C) and the liquid-crysalline phase (50°C). In addition, the mouse body temperature is approximately 41°C. Fig. 4 compares the fluorescence anisotropy of DPH in DPPC liposomes containing Muc1 lipopeptide (400 μg/ml) and Lipid A (200 μg/ml) as a function of cholesterol content. At 22°C, increasing amounts of cholesterol increased the rotational motion of DPH independent of the presence of Lipid A and Muc1 lipopeptide (Fig. 4A). This is expected since cholesterol addition should break up well-ordered domains of DPPC in the gel phase. However, liposomes containing the Muc1 lipopeptide exhibited a greater restriction on the rotational motion of DPH than bilayers composed only of DPPC/cholesterol. Studies at 37°C were similar to those at 22°C (data not shown). Anisotropy measurements obtained at 41°C and 50°C (Fig. 4B,C, respectively) exhibited a threshold at $\sim$20 mol% cholesterol, above which a further decrease in the rotational motion of DPH was evident only for those formulations containing the Muc1 lipopeptide. At these temperatures, increasing amounts of cholesterol should

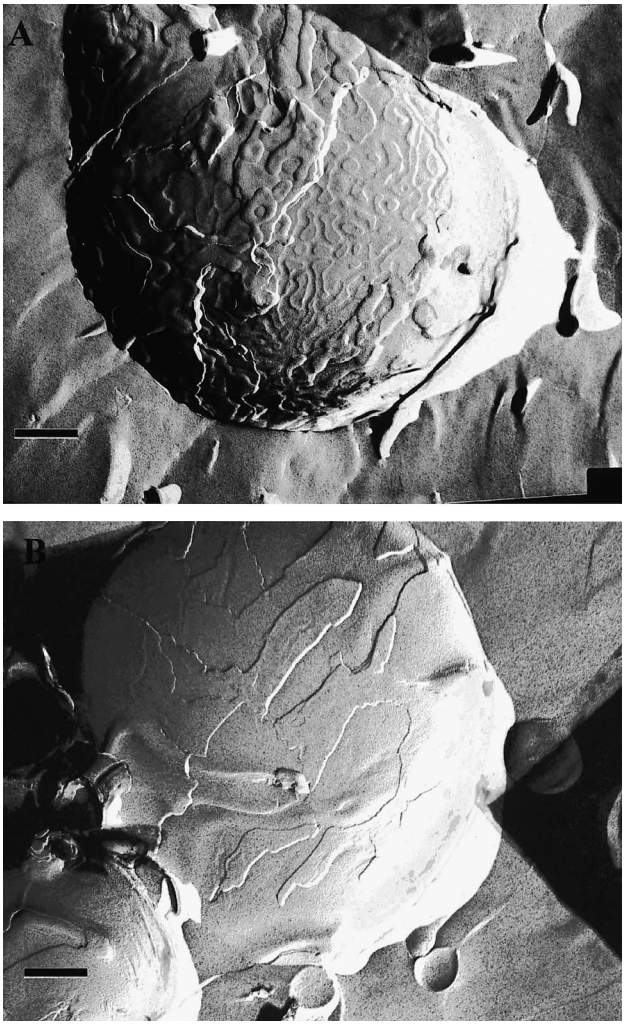

Fig. 3. The effect of Muc1 lipopeptide on the surface appearance of liposomal formulations. All formulations contained 50 mol% cholesterol. (A) Liposomes containing 400 μg/ml Muc1 lipopeptide and no Lipid A. (B) Liposomes containing 200 μg/ml Lipid A and no Muc1 lipopeptide. Freeze-fracture was performed on formulations warmed to room temperature. Bar = 250 nm.

result in a uniform liquid-ordered phase [16,17]. Such a state is seen most clearly in the control liposomes at 50°C (Fig. 4C, dotted line). The differences in anisotropy at all temperatures appeared to be dependent on Muc1 lipopeptide and not Lipid A (see data for 50 mol% cholesterol, Fig. 4A–C). These data may suggest the formation of Muc1 lipopeptide-rich microdomains which are thermally labile at lower cholesterol levels. Such microdomains may be immiscible in a liquid-ordered bilayer, which would be prominent at higher cholesterol levels (> 20 mol%). Alternatively, they could be stabilized by a preferential uptake of cholesterol.

The dependence of the rotational motion of DPH on Muc1 lipopeptide was further evaluated by comparing anisotropy data obtained at different concentrations of Muc1 lipopeptide over the range of 0–30 mol% cholesterol and in the absence of Lipid A. Fig. 5 shows data collected at 22°C, 41°C and 50°C. At all three temperatures an increase in Muc1 lipopeptide concentration resulted in a further decrease in the rotational motion of the fluorophore. At 50°C and without Lipid A (Fig. 5C), 10 mol% cholesterol compared to 20 mol% cholesterol in the presence of Lipid A (Fig. 4C), was observed to further decrease the rotational motion of DPH. A 20 mol% cholesterol threshold was apparent at 41°C at 400 and 1000 μg/ml Muc1 lipopeptide (Fig. 5B). The higher choles-

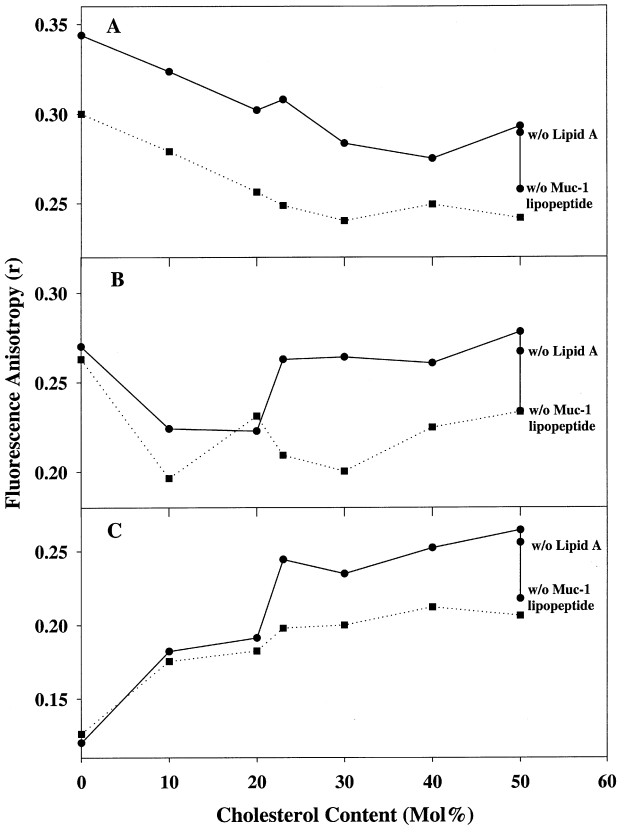

Fig. 4. Fluorescence polarization anisotropy profiles as a function of cholesterol content. Solid lines denote liposomal formulations containing 400 μg/ml Muc1 lipopeptide and 200 μg/ml Lipid A (with exceptions as designated in figures). Dotted lines denote control liposomes prepared from DPPC/cholesterol. 22°C (A); 41°C (B); 50°C (C).

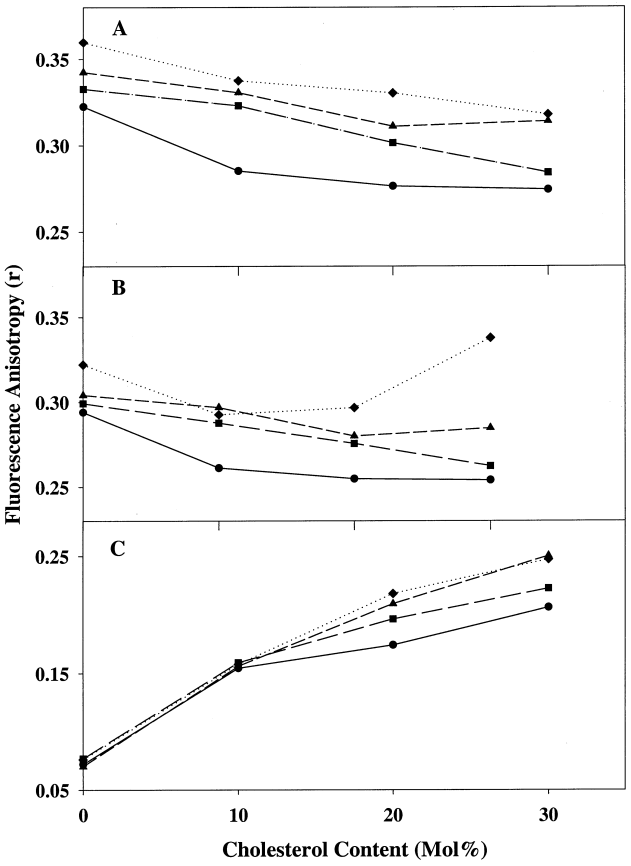

Fig. 5. Fluorescence polarization anisotropy profiles as a function of cholesterol and Muc1 lipopeptide content. All liposomal formulations were prepared from DPPC/cholesterol without Lipid A at four different concentrations of Muc1 lipopeptide: 0 μg/ml (●); 100 μg/ml (■); 400 μg/ml (▲); 1000 μg/ml (♦). (A) 22°C; (B) 41°C; (C) 50°C.

terol threshold at 50°C in the presence of Lipid A suggests that Lipid A has some role in ordering or disordering the liposomal Muc1 vaccine bilayer. Fluorescence anisotropy measurements were also performed on a series of formulations prepared from DPPC/cholesterol/Lipid A, but without Muc1 lipopeptide. At all temperatures studied these formulations were similar to preparations containing DPPC/cholesterol alone (data not shown). Hence, Lipid A did not appear to affect the rotational motion of DPH in the absence of the Muc1 lipopeptide. Moreover, DPPC/cholesterol liposomes formulated with lipopeptide alone still exhibited a decrease in the rotational motion of DPH in conjunction with increasing cholesterol content. These data suggest that Lipid A is not associated with the putative microdomains and may exert a disordering effect that demands higher cholesterol content (20 vs. 10 mol%) to overcome.

The calorimetric heating profiles of liposomal formulations over the range of 0 to 30 mol% cholesterol are shown in Fig. 6. At 0 mol% cholesterol, inclusion of Muc1 lipopeptide and Lipid A significantly decreased the pretransition temperature and enthalpy (38%) and moderately decreased the main phase transition enthalpy (11%) of the DPPC bilayer. Hence, these components destabilized the DPPC gel phase and appeared to disrupt DPPC cooperative units required for the pretransition. The lack of a significant change in the band shape and full width at half height (FWHH) of the main transition band suggests a surface effect. Higher levels of cholesterol preclude the formation of a ripple phase and do not exhibit a pretransition. At 20 mol% cholesterol, the liposomal vaccine formulation exhibited a biphasic

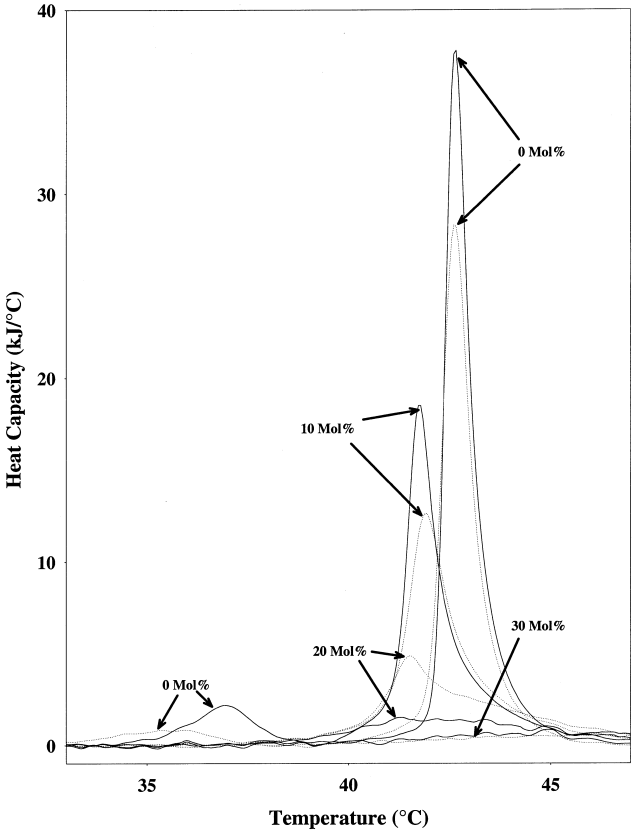

Fig. 6. Differential calorimetry heating profiles at varying amounts of cholesterol. Solid lines denote control liposomes prepared from DPPC/cholesterol. Dotted lines denote liposomal formulations containing 400 μg/ml Muc1 lipopeptide and 200 μg/ml Lipid A. Heating scans were collected at 20°C/h. No pretransition was observed at ≥ 10 mol% cholesterol.

transition and a significant increase in the main phase transition enthalpy compared to control formulations containing only DPPC/Cholesterol (4.2 kcal vs. 2 kcal). The peak shape was biphasic with a sharp lower-temperature component and a broader higher-temperature component. The existence of the sharp and broad components would be consistent with a lateral phase separation due to cholesterol-free and cholesterol-rich domains, respectively [18]. The effect at 20 mol% cholesterol was equivalent to a reduction in cholesterol available to mix with the bulk DPPC. Above cholesterol levels of 30 mol%, differences could not be observed due to the broad transition bands. Hence, DSC, like fluorescence anisotropy and freeze-fracture EM, exhibited a threshold effect of 20 mol% cholesterol. Such an effect is again consistent with a preferred association between cholesterol and the Muc1 lipopeptide, but does not address possible contributions from DPPC and/or Lipid A.

Fig. 7 shows the DSC heating profiles for liposomal formulations containing Lipid A (200 μg/ml) in the absence of lipopeptide over the 0–30 mol% cholesterol range. At 0 mol% cholesterol, Lipid A lowered the pretransition temperature of DPPC bilayers and slightly diminished the main phase transition temperature and enthalpy. Interestingly, without the lipopeptide, the pretransition enthalpy is not significantly reduced (compare to Fig. 6). Lipid A appears to prefer the ripple or liquid-crysalline phase over the gel phase, but does not disrupt DPPC cooperative units required to exhibit a ripple phase. At 10 mol% cholesterol, inclusion of Lipid A resulted in a significant decrease in the main phase transition temperature compared to control liposomes, while above 10 mol% cholesterol, only small decreases in the overall main transition phase enthalpies were observed. Such an effect suggests that in the presence of cholesterol, Lipid A further promotes DPPC bilayer disorder. At low cholesterol levels, inhomogeneities in the bilayer packing arrangement may not accommodate Lipid A. Hence, formation of a liquid-crystalline phase is promoted. These data may also explain why fluorescence anisotropy exhibited a higher cholesterol threshold requirement to decrease the rotational motion of DPH in the presence of Lipid A (Fig. 4C) compared to its absence (Fig. 5C). Moreover, Fig. 7 does not display the biphasic transition

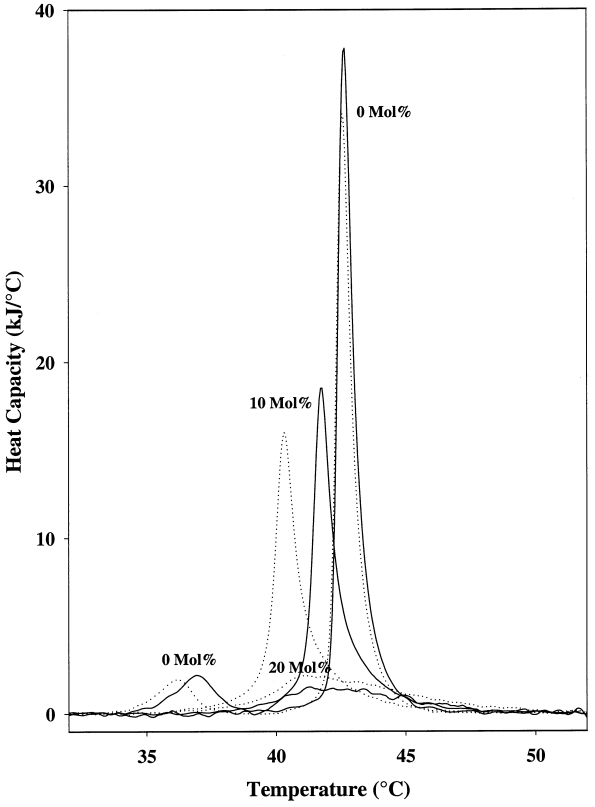

Fig. 7. Differential calorimetry heating profiles at varying amounts of cholesterol (Lipid A contribution). Solid lines denote control liposomes prepared from DPPC/cholesterol. Dotted lines denote liposomal formulations containing 200 μg/ml Lipid A and no Muc1 lipopeptide. Heating scans were collected at 20°C/h.

seen with Muc1 lipopeptide at 20 mol% cholesterol (Fig. 6) suggesting that such an effect is dependent on Muc1 lipopeptide or Muc1 lipopeptide/Lipid A and not Lipid A alone. It also suggests that Lipid A/cholesterol domains do not form and that without the presence of lipopeptide, cholesterol is free to fully interact with the bulk DPPC lipid.

Raman vibrational spectroscopy is particularly sensitive to changes in the intramolecular and intermolecular packing characteristics of the phospholipid bilayer. If lipid microdomains existed due to Muc1 lipopeptide/cholesterol associations, the presence of a more ordered arrangement of DPPC would support the hypothesis that some cholesterol is sequestered from the bulk DPPC molecules. Fig. 8A shows the Raman spectra obtained at 19°C in the C–H stretching region of DPPC bilayers at 20 mol% cholesterol. A significant difference was observed in the presence of Muc1 lipopeptide and Lipid A. Fig. 8B,C show

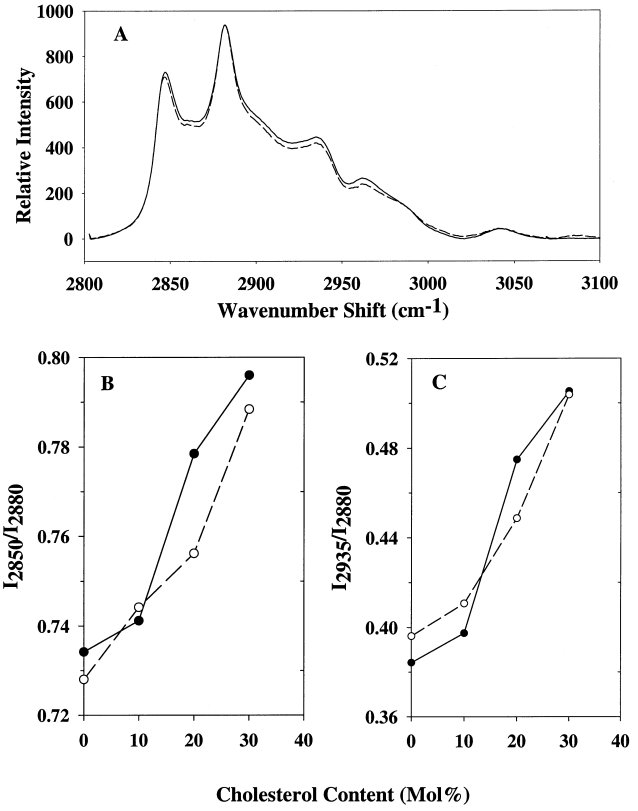

Fig. 8. Raman spectra of control and liposomal vaccine formulations. (A) Comparison of a DPPC/cholesterol control liposome to a vaccine formulation containing 400 μg/ml Muc1 lipopeptide and 200 μg/ml Lipid A, both at 20 mol% cholesterol. (B,C) Calculated Raman order parameters for control and vaccine formulations over the range of 0–30 mol% cholesterol. See text for explanation of the Raman order parameters. Control (solid lines); Muc1 lipopeptide vaccine (dashed lines).

the calculated intramolecular (I_{2930}/I_{2880}) and intermolecular (I_{2850}/I_{2880}) order parameters [19,20] over the range of 0–30 mol% cholesterol. The DPPC bilayers were more ordered at 20 mol% cholesterol when the Muc1 lipopeptide/Lipid A components were included. These data are consistent with an effective decrease in the amount of cholesterol available to the bulk DPPC lipid. Due to the large amount of DPPC present, it remains unclear if DPPC is a component of the putative complex.

4. Conclusions

This study has demonstrated that a peptide-specific cellular immune response (IFN-γ production) in mice inoculated with a Muc1 mucin-based liposomal vaccine was affected by the cholesterol content of the liposomes. Taken together, our results support the formation of Muc1 lipopeptide/cholesterol microdomains analogous to lipid rafts described by other workers [2,21]. Furthermore, they are consistent with liposomal studies showing a link between cholesterol level and both bilayer microviscosity and the magnitude of the primary immune response [3].

Lipid rafts are membrane microdomains formed by the preferential packing of membrane components. For sphingolipid/cholesterol rafts, Simons and Ikonen [2] described a model involving a lateral association due to weak interactions between the carbohydrate headgroups of glycosphingolipids, with cholesterol as a spacer to fill the voids between the associated sphingolipids. The DSC and Raman vibrational spectroscopy data shown in Figs. 6 and 8 suggest that in the presence of lipopeptide some cholesterol was sequestered from the bulk lipid. Hence, this would be consistent with lipopeptide/cholesterol microdomains. The significant but small changes observed in Fig. 8 could be analogous to reports that suggest individual lipids may move in and out of the rafts, which make a sphingolipid-cholesterol cluster difficult to detect spectroscopically [22,23]. Yuan and Johnston [21] used atomic force microscopy to observe lipid raft formation in monolayers composed of physiologically relevant amounts of ganglioside GM1 (a receptor for the cholera toxin) in a DPPC/cholesterol system and found GM1-rich submicron domains ($\sim$100 nm) within the surrounding liquid-ordered phase ($> \sim$30 mol% cholesterol). Interestingly, the freeze fracture data shown in Figs. 2 and 3 exhibits a lipopeptide-dependent surface texture (at $\geq$20 mol% cholesterol), which is also of submicron dimension. Finally, although sphingomyelin is not present, the amide-linked, palmitated Muc1 mucin peptide may preferentially associate with cholesterol. A significant preference for the amide-linkage, sphingomyelins and especially saturated acyl chains was found to be important for association with cholesterol [24]. In addition, prenylated proteins were excluded, while proteins covalently linked to saturated acyl chains were found to incorporate into the cholesterol-rich domains [25].

We hypothesize that a role for the putative Muc1 lipopeptide/cholesterol microdomains may be to influence antigen uptake and processing by the antigen

presenting cells (APC). In this regard, it is noteworthy that Mayor et al. [26] observed a cholesterol-dependent endocytic sorting of glycosylphosphatidylinositol anchored proteins and suggested the involvement of specialized lipid domains or rafts in endocytic sorting. Our observation of a 30 mol% cholesterol threshold for optimal immune response may be due to constraints imposed by the APC membrane composition. For example, typical mammalian cell membranes contain ~20–30 mol% cholesterol. Hence, a higher amount may be required to effect a multimeric aggregation and/or effect antigen uptake or processing by the APC. We note that the formation of these putative microdomains alone was not sufficient for induction of a strong immune response. Lipid A, whose contribution (if any) to the formation of microdomains appeared to be minor, nevertheless was required for a vigorous immune response. Its role may depend on promoting maturation of APCs.

We are currently pursuing studies to test if the cholesterol dependency of the immune response to the vaccine correlates with differences in antigen uptake and processing or alternatively, differences in liposome trafficking to the lymph nodes and spleen. Clearly, the presence of specific microdomains could influence both. To our knowledge, this is the first report suggesting biologically active lipid raft-like structures not involving sphingolipid or ganglioside components in cholesterol rich liposomes.

Acknowledgements

We thank Vicky Kaestner and Linda Xu for their technical assistance and Dr. Fangjun Wu, Mark Thomas and Leane Gadowski for HPLC analysis of the liposomal components. We are grateful to Dr. Jeff Mason for use of the Raman Vibrational spectroscopy system in his lab and the many discussions we shared. We also thank Dr. B. Michael Longenecker for his instructive comments.

References

[1] L. Finegold (Ed.), Cholesterol in Membrane Models, CRC Press, Ann Arbor, MI, 1992.
[2] K. Simons, E. Ikonen, Nature 387 (1997) 569–572.
[3] G.F.A. Kersten, A.M. Van de Put, T. Teerlink, E.C. Beuvery, D.J.A. Crommelin, Infect. Immun. 56 (1988) 1661–1664.
[4] C.M. Cunningham, M. Kingzette, R.L. Richards, C.R. Alving, T.F. Lint, H. Gewurz, J. Immunol. 122 (1979) 1237–1242.
[5] H. Borochov, M. Shinitsky, Proc. Natl. Acad. Sci. USA 73 (1976) 4526–4530.
[6] M. Shinitsky, Dev. Cell. Biol. 4 (1979) 173–181.
[7] G. Gimpl, F. Fahrenholz, Eur. J. Biochem. 267 (2000) 2483–2497.
[8] M.A. Reddish, G.D. MacLean, R.R. Koganty, J. Kan-Mitchell, V. Jones, M.S. Mitchell, B.M. Logenecker, Int. J. Cancer 76 (1998) 817–823.
[9] S.E. Wright, L. Kilinski, S. Talib, K.E. Lowe, J.S. Burnside, J.Y. Wu, N. Dolby, K.E. Dombrowski, J.S. Lebkowski, R. Philip, J. Immunother. 23 (2000) 2–10.
[10] B. Agrawal, S.J. Gendler, B.M. Logenecker, Mol. Med. Today 4 (1998) 397–403.
[11] B. Agrawal, M.A. Reddish, B.M. Logenecker, J. Immunol. 157 (1996) 2089–2095.
[12] R.R. Koganty, M.A. Reddish, B.M. Logenecker, Drug Discov. Today 1 (1996) 190–198.
[13] R.R. Koganty, D. Qui, V. Budzynski, S.S. Gandhi, J.E. Yule, M.A. Reddish, M.J. Krantz, B.M. Logenecker, in: M. Yalpani (Ed.), Biomedical Functions and Biotechnology of Natural and Artificial Polymers, Vol. 3, ATL Press, Shrewsbury, 1996, pp. 105–114.
[14] B.N. Ames, in: E.F Neufeld, V. Ginsburg (Eds.), Methods in Enzymology, Vol. VIII, Academic Press, New York, 1966, pp. 115–117.
[15] J. Huang, J.T. Buboltz, G.W. Feigenson, Biochim. Biophys. Acta 1417 (1999) 89–100.
[16] D.A. Brown, E. London, J. Membr. Biol. 164 (1998) 103–114.
[17] T.P.W. McMullen, R.N. McElhaney, Curr. Opin. Colloid Interface Sci. 1 (1996) 83–90.
[18] R.N.A.H. Lewis, R. McElhaney, in: P. Yeagle (Ed.), The Structure of Biological Membranes, CRC Press, Boca Raton, FL, 1992, pp. 123–125.
[19] I.W. Levin, in: R. Clark, R. Hester (Eds.), Advances in Infrared and Raman Spectroscopy, Vol. 11, Wiley Heyden, New York, 1984, pp. 1–48.
[20] E. Mushayakarara, N. Albon, I.W. Levin, Biochim. Biophys. Acta 686 (1982) 153–159.
[21] C. Yuan, L.J. Johnston, Biophys. J. 79 (2000) 2768–2781.
[22] A. Kusumi, Y. Sako, Curr. Opin. Cell Biol. 8 (1996) 566–574.
[23] M.R. Morrow, D. Singh, D. Lu, C.W.M. Grant, Biophys. J. 68 (1995) 179–186.
[24] B. Ramstedt, J.P. Slotte, Biophys. J. 76 (1999) 908–915.
[25] K.A. Melkonian, A.G. Ostermeyer, J.Z. Chen, M.G. Roth, D.A. Brown, J. Biol. Chem. 274 (1999) 3910–3917.
[26] S. Mayor, S. Sabharanjak, F.R. Maxfield, EMBO J. 17 (1998) 4626–4638.